WEP Warwick Evans Publishing

International Journal of Materials Science and Technology Studies

ISSN: 3006-7693 (Print), ISSN: 3006-3744 (Online) | Volume 2, Number 2, Year 2024
DOI: https://doi.org/10.62051/ijmsts.v2n2.02
Journal homepage: https://wepub.org/index.php/IJMSTS/index

Effect of Rare Earth Element Sm on Elastic Modulus and Crack Suppression of Cobalt-Based Alloys in Laser Cladding Applications

Weibo Li *, Yong Yang, Kai Han

College of Mechanical and Automotive Engineering, Qingdao University of technology, Qingdao, 266000, China

*Corresponding Author: Weibo Li

ABSTRACT

In the application of laser cladding technology, cobalt-based alloys are widely used due to their excellent wear resistance and corrosion resistance. However, they are prone to cracking under high-temperature conditions, which limits their application range. To address this issue, this study introduced the rare earth element Sm into cobalt-based alloy powders and systematically investigated its effect on crack suppression in cobalt-based alloys. The results indicate that with the increase in Sm content, the elastic modulus of the cobalt-based alloy first increases and then decreases. When the Sm content is 10%, the alloy achieves its maximum nano-hardness and elastic modulus, but the crack suppression effect is the weakest at this point. As the Sm content further increases to 30%, the cracks are significantly reduced, and the overall performance of the material is markedly improved. In conclusion, this study successfully developed a cobalt-based alloy coating with excellent performance and fewer cracks, providing an important reference for the application of laser cladding technology.

KEYWORDS

Laser cladding; Cobalt base alloy; Rare earth elements; Crack suppression; Nano-indentation hardness; Elasticity modulus

1. INTRODUCTION

Laser cladding technology, as an efficient surface enhancement method, has been widely applied in mechanical, energy, and aerospace fields to improve the wear resistance, corrosion resistance, and oxidation resistance of metal substrates. Iron-based alloys are an important choice for laser cladding coatings due to their excellent mechanical properties, lower cost, and high wear resistance. However, despite the exceptional wear and corrosion resistance of cobalt-based alloys, the rapid heating and cooling during the laser cladding process can lead to stress concentration, resulting in crack formation that severely affects the service life and reliability of the cladding layer.

To address these issues, researchers have introduced various trace elements into iron-based alloys to improve their microstructure properties. Rare earth elements, due to their unique electronic structure and high reactivity, are considered to have potential modifying effects. Among the many rare earth elements, samarium (Sm), as a light rare earth element, has gained significant attention in the field of material modification in recent years due to its unique physical and chemical properties. Research has shown that the appropriate addition of rare earth element Sm can significantly refine the grains, suppress crack propagation, and improve the mechanical properties of the material.

In the application of laser cladding iron-based alloy coatings, the elastic modulus is a crucial indicator for measuring a material's resistance to elastic deformation, directly affecting the coating's load-bearing capacity and stability under various operating conditions. As an additive element, samarium (Sm) may influence the elastic modulus of iron-based alloys by altering the microstructure of the matrix. However, research on the effect of Sm on the elastic modulus of iron-based alloys and its role in crack suppression is still insufficient, particularly under laser cladding process conditions, and its specific impact mechanisms need further exploration.

Therefore, this study aims to systematically investigate the effects of adding the rare earth element Sm to laser-cladded iron-based alloys through experiments and analysis. The focus will be on studying its impact on the alloy's elastic modulus and its potential mechanisms for crack suppression. Through a comprehensive analysis of microstructure, crack behavior, and mechanical properties, this study seeks to provide theoretical and technical support for the application of rare earth elements in the field of laser cladding.

2. EXPERIMENTAL EQUIPMENT AND PROCESS OF LASER CLADDING

2.1. Experimental Equipment

The laser cladding layer formation system is illustrated in Fig. 1(a). The laser is a FL020 fiber laser produced by the German company ROFIN, with a maximum output power of 2 kW. The laser beam is circular, and the desired beam diameter is set by adjusting the distance between the laser head and the substrate. The laser is integrated into a 6-axis industrial robot produced by the German company KUKA. During the laser cladding process, the cladding layer is formed by controlling the robot's motion parameters.

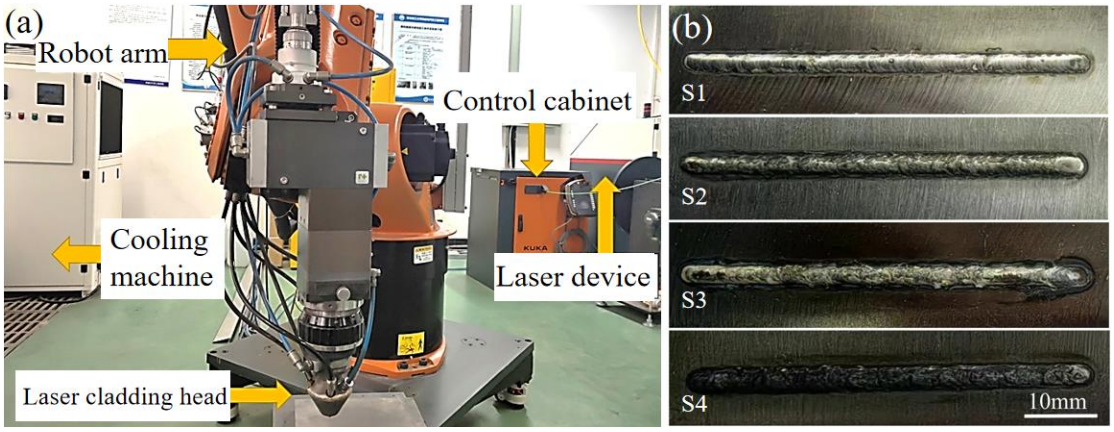

Figure 1. (a) Laser cladding equipment; (b) Laser cladding coating sample

2.2. Experimental Material

The base material chosen is tempered 42CrMo steel plates with dimensions of 60×15×10 mm. The material composition and content are listed in Table 1. Prior to the laser cladding process, the base surface is treated to remove rust and dust using metallographic sandpaper and anhydrous ethanol cleaning. The cladding material is a composite laser cladding powder made from spherical iron-based alloy powder (B 12 wt%, C 1.0 wt%, Cr 5.0 wt%, Fe 30 wt%, Co Bal) mixed with Sm powder in specific mass fractions through ball milling, as detailed in Table 1.

Table 1. Composition and content of 42CrMo matrix material (wt.%)

C	Cr	Mo	Mn	Si	Fe
0.39	0.92	0.19	0.62	0.18	Bal.

Table 2. Laser cladding material ratio (wt.%)

Number	Co-base alloy powder	Sm
S1	100	0
S2	90	10
S3	80	20
S4	70	30

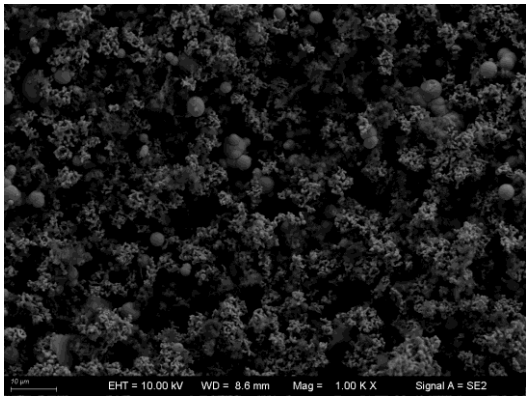

Figure 2. Morphology of composite cladding materials

2.3. Experimental Procedure

Firstly, the prepared powder is ball-milled for 2 hours. Prior to the experiment, the powder is dried in an oven at 120°C for 2 hours. The morphology of the composite cladding powder is shown in Fig. 2. In this experiment, a fiber laser is used for single-pass laser cladding, with laser power, scanning speed, and laser spot diameter chosen as the main process parameters. The thickness of the pre-coated powder is set between 0.8 mm and 1.2 mm. The laser power is set to 1000 W, the scanning speed is set to 3 mm/s, and the laser spot size is set to 3 mm. During the laser cladding process, high-purity argon gas is used as the protective gas to prevent oxidation of the melt pool. The morphology of the powder after laser cladding is shown in Fig. 1(b).

2.4. Materials Characterization

After the cladding is completed, the samples are cut into suitable sizes of 10×15×10 mm using a wire cutting machine for ease of observation. Before observation, the cladding layer samples are subjected to grinding and polishing. The cross-sections are then subjected to nanoindentation measurements to test the changes in elastic modulus of the cladding layer with varying Sm content.

For SEM observation, the samples are first ground with metallographic paper up to 2000#. They are then mechanically polished using a polishing agent and cloth on a metallographic polishing machine until the surface achieves a mirror finish. The polished samples are etched with aqua regia (concentrated HNO_3: concentrated HCl = 1:3), then cleaned with anhydrous ethanol, and dried with a blower before observing the cladding layer's microstructure. Scanning Electron Microscopy (SEM) is used to examine the microstructural features and defects such as cracks, while Energy Dispersive Spectroscopy (EDS) is employed for elemental analysis of selected areas.

3. RESULTS AND DISCUSSION

3.1. Macroscopic Appearance of the Coating

Fig. 3 shows the macroscopic appearance of the cross-sections of four sample groups with different Sm contents. After completing the laser cladding experiments, the cross-sections of these samples were observed using SEM. The results indicate that as the content of the rare earth element Sm increases, the occurrence of cracks decreases significantly. Fig. 3(a) shows the cladding layer without Sm addition, where a crack extends through the entire layer, severely affecting the overall performance of the cladding. When the Sm content is increased to 10%, the crack width decreases, but several fine cracks extending outward are observed, indicating that the addition of rare earth elements has a noticeable effect on crack suppression. With further increase of Sm content to 20%, Fig. 3(c) shows a more flattened macroscopic appearance of the cladding layer, with reduced dilution rate, indicating better bonding with the substrate. Although a finer crack appears on the top of the cladding layer, the overall quality improves significantly. When the Sm content reaches 30%, Fig. 3(d) shows that the cladding layer is in excellent condition with a smooth surface and no cracks, indicating that cracks are well suppressed. The rare earth element Sm demonstrates a significant crack-suppressing effect on cobalt-based alloys. Further studies will be conducted to explore the mechanism behind Sm's effect on crack suppression in cobalt-based alloys.

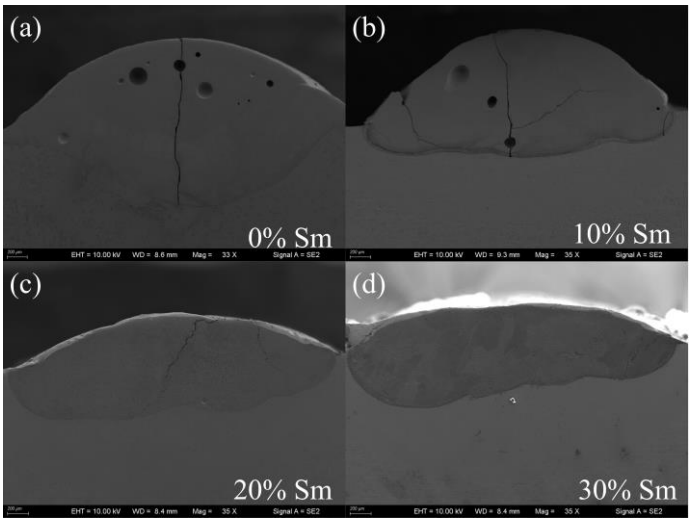

Figure 3. Macro profile of cladding layer with different Sm content

3.2. Elastic Modulus and Nanohardness of Coating

Nanoindentation tests were conducted on samples with different Sm contents (0 wt.%, 10 wt.%, 20 wt.%, 30 wt.%) to obtain their nanoindentation hardness and elastic modulus. Fig. 4 shows the results of the elastic modulus at different Sm contents. It was found that the elastic modulus is highest at 10% Sm content, indicating the smallest elastic deformation capacity. When internal stress exceeds the material's elastic strain capacity, cracks in the cladding layer are likely to form. As the Sm content increases, the elastic modulus first increases and then decreases, with 10% serving as a turning point. Between 10% and 30%, the elastic modulus decreases. A smaller elastic modulus suggests that the alloy coating can endure greater deformation, thus resisting stress concentration during the cladding process and suppressing crack formation.

Combining with the nano-hardness results shown in Fig. 5, it is evident that the coating has the highest nano-hardness and elastic modulus at 10% Sm content. A higher elastic modulus means less deformation capacity, making the material less able to withstand higher stresses and leading to crack

formation. This also explains why the S4 sample mentioned earlier has the fewest or even no cracks, as it has the smallest elastic modulus.

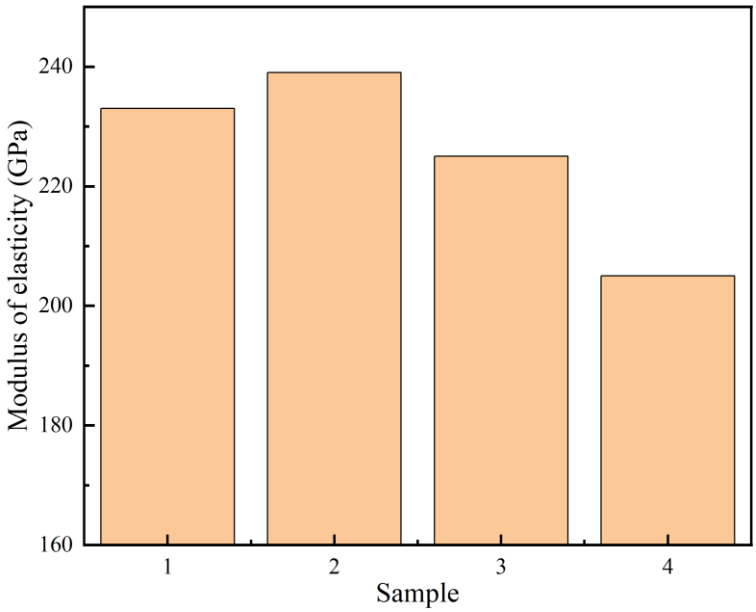

Figure 4. Test results of elastic modulus with different Sm content

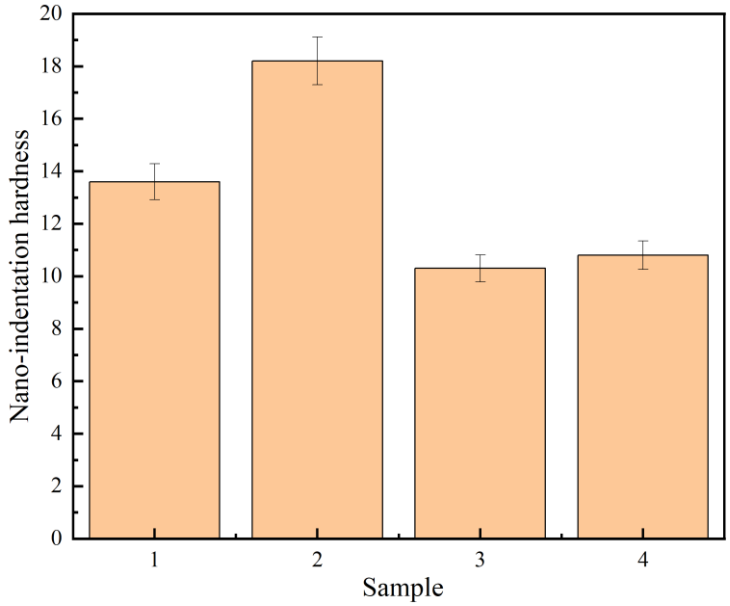

Figure 5. Nanohardness test results with different Sm content

3.3. Analysis of Microscopic Appearance of Coating

Fig. 6 presents the EDS elemental mapping results for cracks in the S1 coating (0% Sm content). The image shows a relatively high concentration of C and O elements at the crack sites, which may be attributed to element segregation leading to the accumulation of C. This localized increase in brittleness contributes to crack formation. Fig. 7 displays the EDS elemental mapping results for cracks in the S3 coating (20% Sm content). Compared to the S1 coating, there is a significant reduction in the concentration of C and O elements at the crack sites. The comparison between Fig. 6 and 7 clearly demonstrates that the increase in Sm content effectively prevents element segregation.

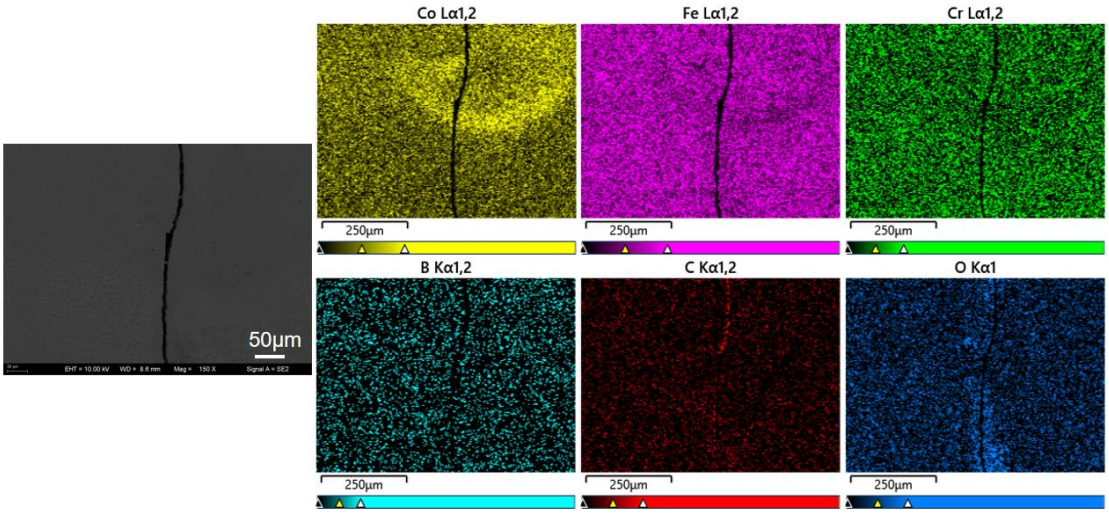

Figure 6. EDS element scanning analysis results of cracks in S1 coating (0wt.%Sm)

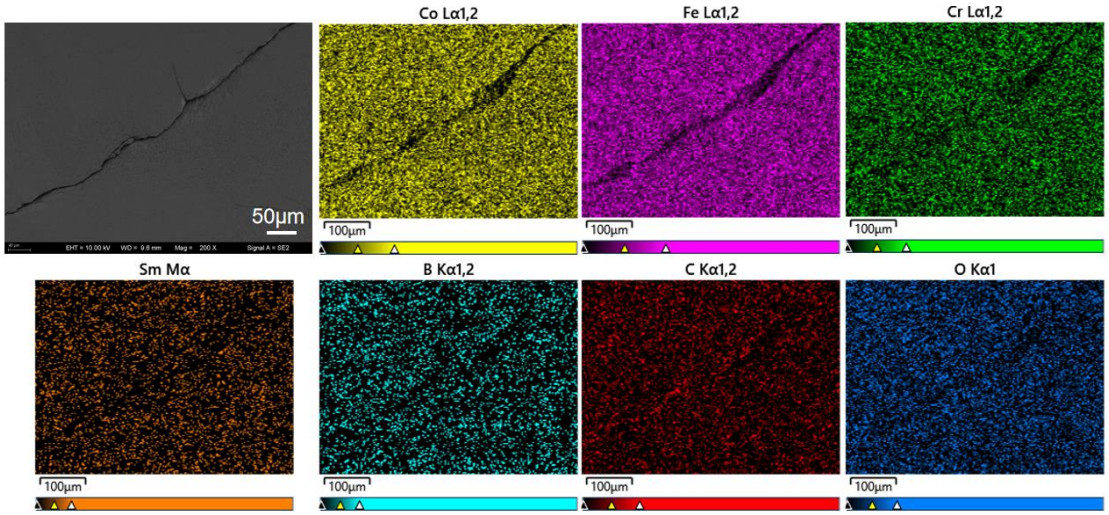

Figure 7. EDS element scanning analysis results of cracks in S3 coating (20wt.%Sm)

4. CONCLUSION

In this study, cobalt-based alloy coatings were prepared on a 42CrMo substrate, and the effect of different Sm contents on crack suppression was investigated. The findings are as follows:

The rare earth element Sm has a significant effect on suppressing cracks in cobalt-based alloys. By controlling the elastic modulus, it was observed that a higher elastic modulus is associated with a higher likelihood of crack formation, while a lower elastic modulus corresponds to fewer cracks.

As the Sm content increases, the elastic modulus initially increases and then decreases. When the Sm content is below 10%, increasing Sm content results in higher nano-hardness and elastic modulus of the coating. However, when the Sm content exceeds 10%, the elastic modulus decreases with increasing Sm content.

CONFLICTS OF INTEREST

The authors declare that they have no known competing financial interests or personal relationships that could have appeared to influence the work reported in this paper.

REFERENCES

[1] Haitao Ding, Yue Cao, Ke Hua, Yanlin Tong, Na Li, Linghong Sun, Xiaolin Li, Hongxing Wu, Haifeng Wang. “Fretting wear resistance at ambient and elevated temperatures of 316 stainless steel improved by laser cladding with Co-based alloy/WC/CaF2 composite coating”. Optics & Laser Technology, Vol.163, pp.109428, 2023. https://doi.org/10.1016/j.optlastec.2023.109428

[2] Qin Tan, Kun Liu, Jie Li, Shaoning Geng, Liying Sun, Vladimir Skuratov. “A review on cracking mechanism and suppression strategy of nickel-based superalloys during laser cladding”. Journal of Alloys and Compounds, Vol.1001,pp.175164, 2024. https://doi.org/10.1016/j.jallcom.2024.175164

[3] Changyao Ouyang, Rui Wang, Qiaofeng Bai, Zhi Chen, Xianguo Yan. “Aging strengthening treatment of laser cladding Co-based alloy coating”. Materials Letters, Vol.313, pp.131746, 2022. https://doi.org/10.1016/j.matlet.2022.131746

[4] Shisheng Lu, Lingqian Wang, Jiansong Zhou, Jun Liang. “Microstructure and tribological properties of laser-cladded Co-Ti3SiC2 coating with Ni-based interlayer on copper alloy”. Tribology International, Vol.171, pp.107549, 2022. https://doi.org/10.1016/j.triboint.2022.107549

[5] Huo-ming Guo, Qian Wang, Wen-jian Wang, Jun Guo, Qi-yue Liu, Min-hao Zhu. “Investigation on wear and damage performance of laser cladding Co-based alloy on single wheel or rail material” , Wear, Vol.328–329, pp.329-337, 2015. https://doi.org/10.1016/j.wear.2015.03.002

[6] Zhiyuan Li, Hua Yan, Peilei Zhang, Jialong Guo, Zhishui Yu, Jonas W. Ringsberg. “Improving surface resistance to wear and corrosion of nickel-aluminum bronze by laser-clad TaC/Co-based alloy composite coatings” Surface and Coatings Technology, Vol. 405, pp.126592, 2021. https://doi.org/10.1016/j.surfcoat.2020.126592